ISBN: 978-3-95450-262-2 ISSN: 2673-5350 doi: 10.18429/JACoW-IBIC2025-WEPCO15

INFLUENCE ANALYSIS OF DIPOLE MAGNET DESIGN AND BEAM COLLIMATION IN THE HIGH-PRECISION ENERGY SPECTROMETRY SYSTEM*

Y. Zeng†, D. Xiao†, D. Lu, Y. Wang, H. Hu
Huazhong University of Science and Technology, Wuhan, China
W. Han‡, The Institute of High Energy Physics of the Chinese Academy of Sciences, Beijing, China
K. Liu, T. Hu‡, Huazhong University of Science and Technology, Wuhan, China

Abstract

The high-precision energy spectrometry system, as a key electron beam diagnostic, enables accurate measurement of beam energy distribution and supports injector performance optimization. Beam collimation prior to the system affects measurement accuracy. For electron injectors operating at a few MeV, a high-precision spectrometry system based on the magnetic deflection method is developed, and an energy spectrum model is established to study the design and magnetic field optimization of the key dipole magnet (D-magnet) as well as the influence of upstream beam collimation on beam trajectory accuracy. Simulation results indicate that the optimized D-magnet enhances performance, and beam collimation analysis verifies effective trajectory control, improving system precision and providing technical support for high-precision energy measurements.

INTRODUCTION

The high-precision energy spectrometry system is employed to measure core electron beam parameters, including energy and energy spread, and to support injector performance optimization in facilities such as free-electron lasers [1, 2], colliders [3, 4], synchrotron light sources [5], and ultrafast electron diffraction systems [6]. For linear accelerators below 20 MeV, used in industrial and medical applications [7–11], accurate beam energy measurement is essential for ensuring both injector output quality and downstream system performance.

Among common beam energy diagnostic methods [12–17], compared with the time-of-flight method, which is characterized by strong energy dependence, the Compton backscattering and synchrotron radiation measurement methods, which are constrained by the need for modification of the original beamline, and the range measurement method, which is limited by slow measurement speed, the D-magnet-based energy analysis method is favored due to its simplicity, ease of implementation, and high resolution. However, this method is dependent on the design quality of the D-magnet and the theoretical description of beam transport, and it is also influenced by deviations in beam alignment during transport.

* Work supported by the National Key R & D Program of China (No.2024YFA1612200) and the National Natural Science Foundation of China (No.12341501).
† Equal contribution
‡ hanwj@ihep.ac.cn, TongningHu@hust.edu.cn

Based on the compact low-energy injector experimental platform under development at Huazhong University of Science and Technology [18], which is designed for the measurement of key parameters of 3–15 MeV electron beams, the D-magnet has been subjected to an optimized design, and the upstream beam collimation system has been analyzed.

PRINCIPLE AND DESIGN OF THE ENERGY SPECTROMETRY SYSTEM

The energy spectrometry system, based on magnetic deflection, consists of a D-magnet, drift sections, and a measurement screen. In Fig. 1, the spectrometry system with beam collimation is shown, where the electron bunch is corrected and introduced into the system.

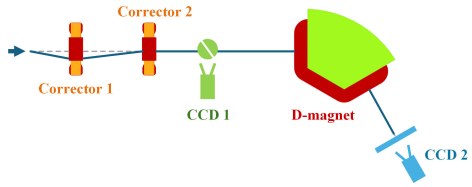

Figure 1: The spectrometry system with beam collimation.

Due to the Lorentz force, electron beams with different energies E and longitudinal distributions are deflected along distinct trajectories when subjected to the magnetic field B of the D-magnet:

$$E = \sqrt{(B\rho ec)^2 + m_0^2 c^4}, \tag{1}$$

where ρ is the radius of curvature, c, e, and m_0 are the speed of light, electron charge, and electron mass, respectively.

On this platform, the energy spectrometry system is designed for point-to-point imaging, with a slit at the entrance to ensure the target distribution reflects the electron bunch energy spread ES.

$$ES = \frac{\left(1+\gamma^{-1}\right)}{m_{13}} \sqrt{\langle x_1^2\rangle - m_{11}^2 \langle x_0^2\rangle}, \tag{2}$$

where $\gamma = \frac{E}{E_0}$ denotes the Lorentz factor, E_0 is the electron rest energy. The variable x represents the horizontal position, with the subscripts 0 and 1 referring to the entrance and exit parameters of the system, respectively. The quantities

ISBN: 978-3-95450-262-2 ISSN: 2673-5350 doi: 10.18429/JACoW-IBIC2025-WEPCO15

m_{11} and m_{13} are elements of the three-dimensional transfer matrix of the system. The symbol <> indicates the mean value.

The D-magnet with a bending angle of 60° and a bending radius of 0.3 m is selected for analysis. To design the system such that $|m_{11}|$ is minimized and $|m_{13}|$ is maximized, while maintaining a compact layout, the drift length downstream of the spectrometer magnet is set to 0.45 m, and the drift length from the system entrance to the magnet entrance is set to 0.6069 m.

DESIGN AND SIMULATION ANALYSIS OF THE D-MAGNET

A C-shaped sector dipole magnet was chosen based on the aforementioned considerations and [18] design parameters. Unlike bulky H- and frame-type magnets, C-type magnets offer greater flexibility and integration while avoiding high-field limitations and sextupole components [19].

Design Analysis of the D-Magnet

The pole and yoke are composed of high-permeability soft magnetic materials, resulting in most of the magnetomotive force being dropped across the air gap, and the per-pole excitation current can thus be preliminarily estimated using Eq. (1):

$$F(E) = NI = f\frac{B_\delta g}{2\mu_0} = f\frac{\sqrt{E^2 - E_0^2}\,g}{599.585\,\rho\,\mu_0}, \tag{3}$$

where NI represents the excitation current per pole, g is the gap height, and μ_0 is the vacuum permeability. Both E and E_0 are expressed in units of MeV. The factor $f = 1.05 \sim 1.10$ is introduced to account for magnetic losses in the magnet. With the air gap of $g = 0.04$ m and $f = 1.05$, the excitation current increment is calculated as $\Delta NI = F(E + \Delta T) - F(E) = 18.59$ A, ensuring 0.1 MeV energy precision within the measurement range.

Meanwhile, to account for magnetic flux leakage [20], the pole width is extended laterally to ensure the required field uniformity $\frac{\Delta B}{B_0}$ is achieved within the working region. Based on the requirement, the extension distance c_1 is preliminarily estimated as follows:

$$\frac{2c_1}{g} = 0.75 - 0.36\ln\left(100\frac{\Delta B}{B_0}\right). \tag{4}$$

The pole face width is determined to be ~180 mm. Finally, the D-magnet is designed as shown in Fig. 2(a).

Shimming and Chamfering Analysis of the D-Magnet

The pole faces are shimmed and chamfered to optimize the magnetic field distribution. The resulting central and integrated fields under a power supply current $I = 10$ A , are shown in Fig.2(b), with the longitudinal field distribution presented in Fig.2(c).

After shimming and chamfering, the transverse field uniformity of the magnet is improved from 3.853E-4 to 3.799E-4, and the integrated field uniformity is improved from 8.896E-4 to 4.316E-04. The central field decreases slightly with transverse position due to the C-type yoke, but the variation remains within 1.5 Gs.The maximum absolute errors of the field and integrated field, 3.421E-4 and 3.446E-4, both satisfy the 5.0E-4 requirement.

Simultaneously, the 3D magnet field is analyzed via elliptical multipole expansion [21], which better fits the yoke and aperture geometry than circular expansion, with reduced multipole contributions after shimming, as shown in Table 1.

Table 1: Comparison of Multipole Component Ratios Before and After Magnet Shimming and Chamfering

	B3/B1	**B5/B1**	**B7/B1**	**B9/B1**
Pre	7.918E-4	1.569E-3	1.050E-3	1.032E-3
Post	2.140E-4	4.387E-4	2.758E-4	5.252E-4

ANALYSIS OF BEAM COLLIMATION

To ensure accurate energy spectrometry and minimize fringe field effects, the beam must be precisely maintained within the magnet's mid-plane. While mechanical alignment can achieve millimeter-level precision, electromagnetic correction is essential for high-precision measurements to further enhance trajectory control. On this platform, dipole magnetic fields are generated using Corrector 1 and Corrector 2 to collimate the beam prior to entering the energy spectrometry system.

A preliminary evaluation of the collimation system on the platform is conducted, and beam collimation is simulated using the beam dynamics software Astra [22]. Initial trajectory deviations of bunch are randomly generated, and trajectory correction is achieved by adjusting the magnetic flux density of the corrector magnets, as shown in Fig. 3. The results indicate that effective correction is possible when the transverse displacement of the bunch after a 0.3 m drift is less than 2.7 mm, allowing the bunch to enter the high-precision energy spectrometry system in a parallel configuration.

CONCLUSION

Through D-magnet optimization and beam collimation analysis, effective trajectory control and improved precision are achieved, contributing to the development of the injector platform at Huazhong University of Science and Technology.

ACKNOWLEDGMENTS

This work was supported by the National Key R & D Program of China (No.2024YFA1612200) and the National Natural Science Foundation of China (No.12341501).

ISBN: 978-3-95450-262-2 ISSN: 2673-5350 doi: 10.18429/JACoW-IBIC2025-WEPCO15

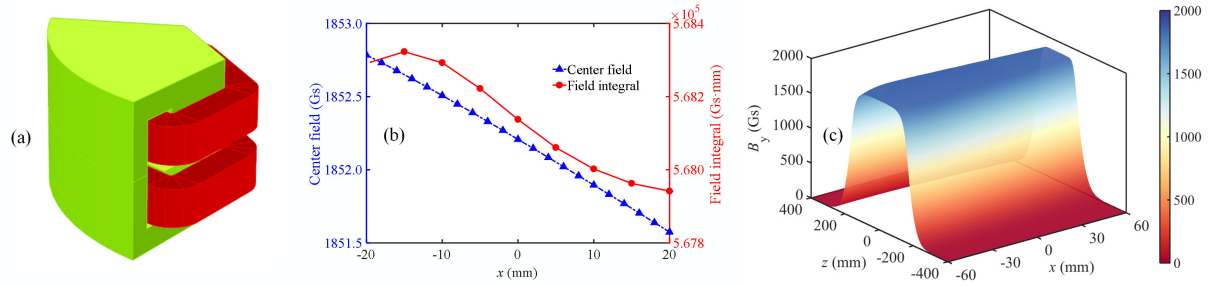

Figure 2: (a) TOSCA 3D simulation [23] of the D-magnet; (b) Simulated central magnetic field and field integral at different transverse positions within the good-field region; (c) Simulated longitudinal field distribution.

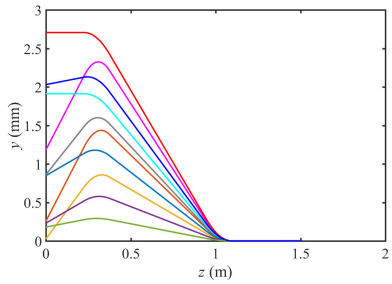

Figure 3: Simulation of beam collimation.

REFERENCES

[1] E. Prat, *et al.*, "High-resolution dispersion-based measurement of the electron beam energy spread", *Phys. Rev. Accel. Beams*, vol. 23, no. 9, p. 090701, 2020. doi:10.1103/PhysRevAccelBeams.23.090701

[2] H. Qian, *et al.*, "Slice energy spread measurement in the low energy photoinjector", *Phys. Rev. Accel. Beams*, vol. 25, no. 8, p. 083401, 2022. doi:10.1103/PhysRevAccelBeams.25.083401

[3] K. Hiller, *et al.*, "ILC beam energy measurement based on synchrotron radiation from a magnetic spectrometer", *Nucl. Instrum. Methods Phys. Res. A*, vol. 580, no. 3, pp. 1191-1200, 2007. doi:10.1016/j.nima.2007.06.027

[4] P. A. Piminov *et al.*, "VEPP-4M Collider Operation at High Energy", in *Proc. IPAC'21*, Campinas, Brazil, May 2021, pp. 155–158. doi:10.18429/JACoW-IPAC2021-MOPAB034

[5] S. A. Antipov, *et al.*, "Design of a prototype laser-plasma injector for an electron synchrotron", *Phys. Rev. Accel. Beams*, vol. 24, no. 11, p. 111301, 2021. doi:10.1103/PhysRevAccelBeams.24.111301

[6] Y. W. Parc, "A Study of the Energy Spread Effect for an Electron Diffraction Experiment", *J. Korean Phys. Soc.*, vol. 55, no. 5, pp. 2247-2251, 2009. doi:10.3938/jkps.55.2247

[7] P. Roy, H. Matthew, S. Heppelmann, S. Upadhyayula, and Z. Harvey, "Review of MeV energy scale accelerators, their capabilities, and common applications", in *Proc. IPAC'24*, Nashville, TN, USA, May 2024, pp. 2036–2039. doi:10.18429/JACoW-IPAC2024-WEPC33

[8] P. Roy, *et al.*, *"Radiological safety aspects of the operation of electron linear accelerators"*, Lawrence Livermore Nat. Lab., Livermore, CA, USA, Rep. LLNL-PROC-2000116, 2024.

[9] T. K. Kroc, "Motivation and Development of a Compact Superconducting Accelerator for X-ray Medical Device Sterilization", Sep. 2022, arXiv:2112.07553 [physics.acc-ph]. doi:10.48550/arXiv.2112.07553

[10] R. Kranzer, *et al.*, "Response of diamond detectors in ultra-high dose-per-pulse electron beams for dosimetry at FLASH radiotherapy", *Phys. Med. Biol.*, vol. 67, no. 7, p. 075002, 2022. doi:10.1088/1361-6560/ac5d2b

[11] A. Vignati, *et al.*, "Beam monitors for tomorrow: the challenges of electron and photon FLASH RT", *Front. Phys.*, vol. 8, p. 375, 2020. doi:10.3389/fphy.2020.00375

[12] I. P. Karabekov and R. Rossmanith, "High accuracy beam energy measurement for linear and circular accelerators", *Nucl. Instrum. Methods Phys. Res. A*, vol. 321, no. 1-2, pp. 18-20, 1992. doi:10.1016/0168-9002(92)90731-8

[13] E. V. Abakumova, *et al.*, "The beam energy measurement system for the Beijing electron–positron collider", *Nucl. Instrum. Methods Phys. Res. A*, vol. 659, no. 1, pp. 21–29, 2011. doi:10.1016/j.nima.2011.08.001

[14] A. Paulus, *et al.*, "Novel time-of-flight electron spectrometer optimized for time-resolved soft-x-ray photoelectron spectroscopy", *Rev. Sci. Instrum.*, vol. 77, no. 4, 2006. doi:10.1063/1.2179419

[15] E. V. Abakumova, *et al.*, "A system of beam energy measurement based on the Compton backscattered laser photons for the VEPP-2000 electron–positron collider", *Nucl. Instrum. Methods Phys. Res. A*, vol. 744, pp. 35–40, 2014. doi:10.1016/j.nima.2014.02.008

[16] P. Klag, *et al.*, "Novel optical interferometry of synchrotron radiation for absolute electron beam energy measurements", *Nucl. Instrum. Methods Phys. Res. A*, vol. 910, pp. 147–156, 2018. doi:10.1016/j.nima.2018.03.063

[17] D. J. McLaughlin, *et al.*, "Permanent-magnet energy spectrometer for electron beams from radiotherapy accelerators", *Med. Phys.*, vol. 42, no. 9, pp. 5517–5529, 2015. doi:10.1118/1.4922230

[18] T. N. Hu, Y. F. Zeng, and K. F. Liu, "Design Considerations of a Magnet-Based Diagnosis System With Compact Layout for Typical Beam Injector", *IEEE Trans. Appl. Supercond.*, vol. 34, no. 5, pp. 1–5, 2024. doi:10.1109/TASC.2024.3355359

ISBN: 978-3-95450-262-2 ISSN: 2673-5350 doi: 10.18429/JACoW-IBIC2025-WEPCO15

[19] T. Zickler, "Basic design and engineering of normal-conducting, iron-dominated electromagnets", Mar. 2011, arXiv:1103.1119 [physics.acc-ph]. doi:10.48550/arXiv.1103.1119

[20] S. Blitz and R. Molloy, "Fringe Field Effects on Bending Magnets, Derived for TRANSPORT/TURTLE", Feb. 2024, arXiv:1310.8630 [physics.acc-ph]. doi:10.48550/arXiv.1310.8630

[21] P. Schnizer, *et al.*, "Theory and application of plane elliptic multipoles for static magnetic fields", *Nucl. Instrum. Methods Phys. Res. A*, vol. 607, no. 3, pp. 505–516, 2009. doi:10.1016/j.nima.2009.06.030

[22] ASTRA: a space charge tracking algorithm, 2017, https://www.desy.de/~mpyflo/.

[23] Opera, 2020, https://www.3ds.com/products/simulia/opera.